

## Numerical Simulation of Electrostatic Jet Atomization Using VOF Method

Mortaza Rahimzadeh<sup>1</sup>, Mohammad Passandideh Fard<sup>2</sup> and Sajad Pooyan<sup>3</sup>

<sup>1</sup>Graduate Student, Ferdowsi University of Mashhad; mortaza\_rahimzadeh@yahoo.com

<sup>2</sup>Associate Professor, Ferdowsi University of Mashhad; mpfard@um.ac.ir

<sup>3</sup>Graduate Student, Ferdowsi University of Mashhad; sajad.pooyan@gmail.com

### Abstract

The atomization of a liquid jet under electrostatic field is numerically simulated using Volume-of-Fluid (VOF) method. In this phenomenon, an electrified liquid is dispersed to fine droplets by an electrostatic force acting on the charged surface of the liquid. The simulations performed in this study correspond to a transient liquid jet leaving a capillary tube maintained at a high electric potential. The Navier-Stokes equations are solved to find the velocity and pressure fields. The surface profile of the deforming jet is defined using the VOF scheme and the advection of the liquid free-surface is performed using Youngs' algorithm. Surface tension force is treated as a body force acting on the free-surface; the method used for this purpose is the continuum surface force (CSF). To calculate the effect of the electric field on the shape of the free-surface, the electrostatic potential is solved first. Next, the surface density of the electric charge and the electric field intensity are computed, and then the electric force is calculated. Liquid is assumed to be a perfect conductor, thus the electric force only acts on the liquid free-surface; the computational method for treating this force is similar to that of the surface tension using the CSF method. The main achievement of this study is the development and validation of a method to obtain electrostatic force distribution on free surface of a conductive fluid and integration of this method into the VOF scheme in order to predict the behavior of the flows with free surface under the effect of an electric field.

**Keywords:** Electrostatic atomization, Irregular domain, VOF, Free surface, Electrostatic force

### Introduction

Electrostatic atomization, also called Electrospray, is a well known phenomenon in which an electrostatic force elongates the liquid meniscus formed at the outlet of a capillary nozzle to a jet which next disrupts into small droplets by electrical and mechanical forces.

Electrospray systems have several advantages over mechanical atomizers. The size of electrospray drops can range from hundreds of micrometers down to several tens of nanometer. The size distribution of the droplets can be nearly monodisperse. Droplet generation and droplet size can be controlled roughly via the control of the flow rate of the liquid and the applied voltage at the capillary nozzle. The fact that the droplets are electrically charged facilitates the control of their motion (including their deflection and focusing) by

means of an electric field. Charged droplets are self dispersing in space, also resulting in the absence of droplet coagulation. The deposition efficiency of a charged spray on an object is higher than that of an uncharged spray. This feature can be utilized, for example, in surface coating or thin-film production.

Electrospray has opened new routes to nanotechnology. Electrospray is used for micro and nano-thin-film deposition, micro or nano-particle production, and micro- or nano-capsule formation. Thin films and fine powders are (or potentially could be) used in modern material technologies, microelectronics, and medical technology[1]. In spite of these advantageous, this method of atomization has some difficulties to perform. The main difficulty is the existence of many different atomization modes depending on the settings of the process. Jaworek et al. [2] classified ten modes of atomization according to geometrical forms of the meniscus and/or jet. Therefore numerical simulation is an effective method to understand and control the phenomenon.

Many researches contributed to the understanding of the phenomenon by modeling and simulation of the involved processes numerically. Hartman et al. [3] developed a Lagrangian model to predict droplet size and velocity and compared the results with experiment. They improved a physical model to obtain the shape of the liquid cone and jet; the electric fields inside and outside the cone; and the surface charge density on the liquid surface [4]. In their model, a one-dimensional momentum equation was used to simulation the flow field. They claimed that the space charge due to the charged droplets has an influence of about 5 to 7% on the electric field at the cone surface. Hartman et al. [5] also used an analytical model for jet break-up and found that the jet break-up mechanism depends on the ratio of electric normal stress to surface tension stress.

Alfonso et al. [6] modeled electrospray using a hybrid experimental-numerical technique. They proved that the surface charges are always in equilibrium, being the liquid bulk quasi-neutral. They presented a consistent general scaling of all EHD variables involved which are verified by experiment. Fang et al. [7] used a model similar to Hartman's one but solved axisymmetric flow equations and used an adaptive grid generation scheme. Their model didn't consider jet break up. Jun Zeng et al. [8] used VOF method to simulate Taylor cone formation. While previous models could only predict the steady shape of the cone-Jet, by utilizing VOF method, Zeng could capture the transition events

as well. However, they didn't consider jet break up and droplet formation; they also used a semi conductor liquid in their simulations. Orest Lastow et al. [9] performed a simulation similar to Zeng, but they studied conductive fluid atomization. They also didn't consider jet break up and surface tension.

As mentioned above, the main drawback of the available works in the literature is that they only solved for steady state situation of the jet profile and, therefore, did not detect transition events. They were also unable to predict the necessary conditions for achieving this mode. The last two papers solved this problem partly but the jet-break up and surface tension were not included. In this work, we use a VOF scheme to model electrospaying along with considering surface tension and jet-break up. This work can easily be extended to model other atomization modes such as dripping, microdripping and spindle modes.

### Problem Geometry

The configuration of the problem is depicted in "Figure 1" and the dimensions of the parts pointed at by alphabetic indexes are cited at the last column of "Table 1". A conductive liquid jet leaves a capillary nozzle with a constant volume flow rate, the velocity of the fluid at the inlet of the nozzle is  $\vec{V}_{top} = -0.05 \frac{m}{s} \hat{j}$ . The electric voltage applied between nozzle and counter electrode is  $\phi_0 = 3.7KV$

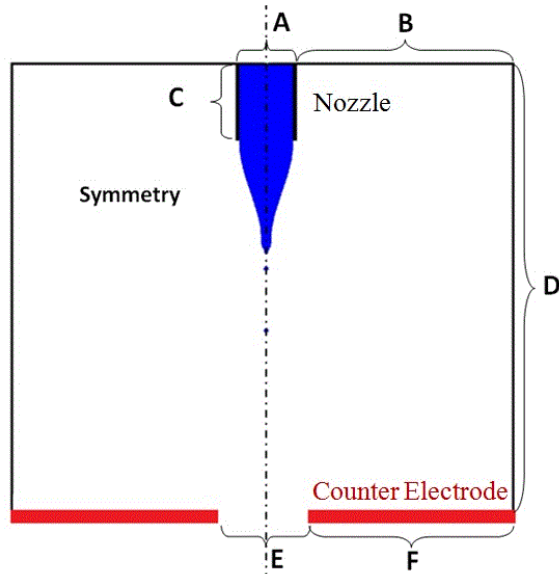


Figure 1 : Configuration of the physical model. Electric potential is applied between the nozzle and the counter electrode. (Figure is not to scale.)

### Governing equations

#### Fluid Flow

The fluid flow is assumed incompressible, axisymmetric, Newtonian and laminar. Because the air surrounding the liquid is not being forced, it does not significantly affect any liquid motion. Therefore, only the liquid phase is considered. The mass and momentum conservation equations are as follows:

$$\vec{\nabla} \cdot \vec{V} = 0 \quad (1)$$

$$\frac{\partial \vec{V}}{\partial t} + \vec{\nabla}(\vec{V}\vec{V}) = -\frac{1}{\rho} \vec{\nabla}p + \frac{1}{\rho} \vec{\nabla} \cdot \vec{\tau} + \vec{g} + \frac{1}{\rho} \vec{F}_b \quad (2)$$

in which,  $\vec{V}$ ,  $\rho$ ,  $p$  and  $\vec{\tau}$  represent the velocity vector, pressure, the liquid density and the stress tensor respectively,  $\vec{g}$  is the gravitational acceleration and  $\vec{F}_b$  is any body force (per unit volume) acting on the fluid. As the fluid is Newtonian the stress tensor is:

$$\vec{\tau} = \mu[(\vec{\nabla}\vec{V}) + (\vec{\nabla}\vec{V})^T] \quad (3)$$

Above equations are solved in order to obtain the flow field. In addition, VOF scheme is used to locate the free surface position. In this method, a scalar function  $f$ , called volume fraction, is defined as the fraction of a cell volume which is occupied by fluid.  $f$  is assumed to be unity when a cell is fully occupied by the fluid and zero for an empty cell. Cells with  $f$  values of  $0 < f < 1$  define the location of free surface. Solving the advection equation for volume fraction as follows,

$$\frac{\partial f}{\partial t} + \vec{V} \cdot \vec{\nabla}f = 0 \quad (4)$$

gives the  $f$  field in each time step.

#### Electrostatic

Along with the hydrodynamic equations presented above, the Laplace equation [10] is solved on the entire domain to calculate the electric potential in every grid cell at each time step:

$$\nabla^2 \phi = 0 \quad (5)$$

In addition, the relation between the electric potential and electric field intensity is known to be:

$$\vec{E} = -\nabla \phi \quad (6)$$

Since the liquid is assumed to be a perfect conductor, the electrostatic force only acts on the liquid free-surface [11]. The electrostatic force per unit area is computed as [12]:

$$\vec{F}_e = \frac{1}{2} \rho_s \vec{E} \quad (7)$$

Where  $\rho_s$  is the surface density of the electric charge and is calculated as:

$$\rho_s = -\epsilon_{Air} \frac{\partial \phi}{\partial n} = -\epsilon_{Air} \vec{E} \cdot \hat{n} \quad (8)$$

Where  $\frac{\partial}{\partial n}$  represents the gradient along the outward normal to the liquid free surface.

#### Boundary Conditions

A Neumann condition is used for pressure in all domain boundaries ( $\frac{\partial p}{\partial n}$ ). Also, an outflow boundary condition is used for velocity on all boundaries except on walls and at the entry of the nozzle where constant velocity is employed. A summary of boundary conditions are mentioned in "Table 1".

Table 1 : Summary of applied boundary conditions based on the schematic shown in Fig. 1.

	Velocity	Pressure	potential	mm
A	$v = Q/A$	$\partial P/\partial n=0$	$\phi = \phi_0$	0.35
B	$\partial u/\partial n=0, \partial v/\partial n=0$	$\partial P/\partial n=0$	$\partial \phi/\partial n=0$	5.65
C	$u = 0, v = 0$	$\partial P/\partial n=0$	$\phi = \phi_0$	1.00
D	$\partial u/\partial n=0, \partial v/\partial n=0$	$\partial P/\partial n=0$	$\partial \phi/\partial n=0$	6.00
E	$\partial u/\partial n=0, \partial v/\partial n=0$	$\partial P/\partial n=0$	$\partial \phi/\partial n=0$	0.70
F	$u = 0, v = 0$	$\partial P/\partial n=0$	$\phi = 0$	5.30

It is important to note that the electric potential of the points within the main flow is equal to applied potential as a result of the perfect conductor assumption for the fluid.

The fluid used in this work is ' water + 0.005 % NaCl ' which its physical properties are listed in "Table 2".

Table 2 : Physical properties of ( water + 0.005 % NaCl )

Density $\rho$ ( $Kg/m^3$ )	Viscosity $\mu$ (Pa.s)	Surface tension $\gamma$ ( $N/m$ )	Relative permittivity $\epsilon_r$	Relaxation time t (sec)
998	$9.9 \times 10^{-4}$	0.0725	87.2	$7.7 \times 10^{-8}$

### Numerical Procedure

The Youngs algorithm [13] is used for advection of function  $f$ . This algorithm consists of two steps: an approximate construction of the free surface and the advection of the interface to a new location. First the interface is reconstructed by locating a line within each interfacial cell utilizing volume fraction of the cell,  $f$ , and normal vector to the interface; normal vectors are computed using  $f$  function gradients in two directions. In the second step the reconstructed interface and new velocities are used to compute volume fluxes across each cell face in one coordinate direction at a time. Having calculated the advection of the interface in all directions, we can compute the final volume fraction field and the new shape of the interface

Surface tension is modeled as a volume force acting on fluid elements near the free surface; the method used is the continuum surface force (CSF) model [14] integrated with smoothed values of function  $f$  in evaluating free surface curvature [15].

The time discretization of the momentum equation is divided into two steps. First, an interim velocity is computed explicitly from convective, viscous, gravitational, and body forces for a time step  $\Delta t$ . Then, the pressure is calculated implicitly. As momentum cannot be advected more than a grid per time step, the Courant number should be less than one. The same condition applied for the volume tracking as it can be only advected to the neighboring cells. Further details of the solution procedure of the hydrodynamic equations using VOF method is given elsewhere [15].

The solution of the electrostatic equations in order to obtain the electrostatic force distribution on the free surface is new in this work and will be explained in details here. Some difficulties arise from constant electric potential throughout the main liquid jet. It

means that the free surface of the liquid is a Dirichlet equation (5) as the value of the electric potential on free surface is known and set to be that of the nozzle. The deforming liquid interface may have any arbitrary shape that doesn't necessarily coincide with the edges of the computational cells. To resolve this issue we use 5 neighboring nodes in different locations with respect to the reconstructed interface to discrete Laplace equation (5) near the free surface. These nodes near the free surface are schematically illustrated in "Figure 2".

By employing a non-uniform Cartesian mesh, equation (5) may be discretized as follows:

$$\frac{2}{A} \left\{ r_R \left( \frac{\phi_{L_{i+1,j}} - \phi_C}{\Delta XR_{i,j} + \Delta XL_{i+1,j}} \right) - r_L \left( \frac{\phi_C - \phi_{R_{i+1,j}}}{\Delta XR_{i-1,j} + \Delta XL_{i,j}} \right) \right\} + \frac{2}{B} \left\{ r_C \left( \frac{\phi_{B_{i,j+1}} - \phi_C}{\Delta YT_{i,j} + \Delta YB_{i,j+1}} \right) - r_C \left( \frac{\phi_C - \phi_{T_{i,j-1}}}{\Delta YT_{i,j-1} + \Delta YB_{i,j}} \right) \right\} = 0 \quad (9)$$

Where:

$$A = \Delta XR_{i-1,j} + \Delta XL_{i,j} + \Delta XR_{i,j} + \Delta XL_{i+1,j} \quad (10)$$

$$B = \Delta YT_{i,j-1} + \Delta YB_{i,j} + \Delta YT_{i,j} + \Delta YB_{i,j+1}$$

and

$$r_C = r_{i,j}$$

$$r_L = r_C - \frac{\Delta XR_{i-1,j} + \Delta XL_{i,j}}{2} \quad (11)$$

$$r_R = r_C + \frac{\Delta XR_{i,j} + \Delta XL_{i+1,j}}{2}$$

$\Delta XL_{i,j}, \Delta XR_{i,j}, \Delta YB_{i,j}$  and  $\Delta YT_{i,j}$  are shown in "Figure 2".

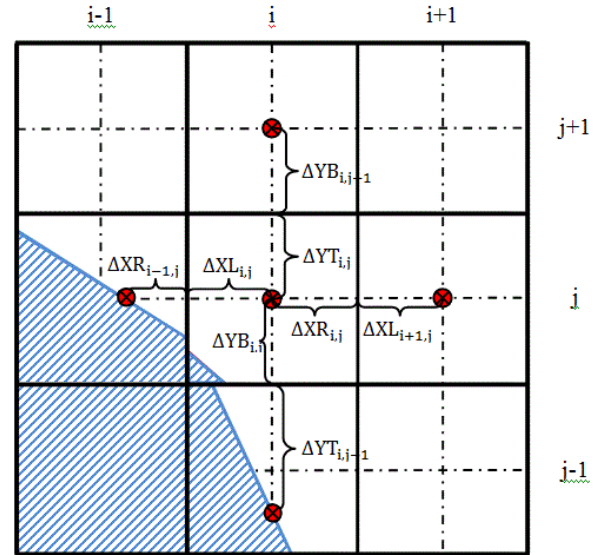


Figure 2 : Nodes (red points) used to discrete the Laplace equation in a sample situation. Geometrical parameters appeared in equation (9) and (10) are also illustrated.

$\Delta XL_{i,j}, \Delta XR_{i,j}, \Delta YB_{i,j}$  and  $\Delta YT_{i,j}$  are parameters computed for each cell near the interface depending on free surface location. As explained before, a boundary condition needs to be satisfied on free surface while solving equation (5), therefore, the above parameters must be calculated in order to exactly locate the

reconstructed free surface profile with respect to the computational grid.

These parameters take different values, depending on the orientation of the interface line in a cell. Nearly ten different arrangements may occur depending on the  $f$  value and the free surface orientation. One of these arrangements in which the interface line intersects both horizontal edges of the cell is illustrated in "Figure 3"; for this case, the parameters are:

$$\begin{aligned} \phi R_{i,j} &= \phi_0 & \phi L_{i,j} &= \phi_0 \\ \phi T_{i,j} &= \phi_{i,j} & \phi B_{i,j} &= \phi_{i,j} \\ \Delta XL_{i,j} &= 0 & \Delta XR_{i,j} &= R \\ \Delta YB_{i,j} &= \frac{\Delta Y_{i,j}}{2} & \Delta YT_{i,j} &= \frac{\Delta Y_{i,j}}{2} \end{aligned} \quad (12)$$

$\phi R$ ,  $\phi L$ ,  $\phi T$  and  $\phi B$  are electric potentials used in discretization of equation (5). If a node selected to discrete the equation lies on the free surface, its value is known and equal to the applied potential  $\phi_0$ , otherwise, it must be calculated.

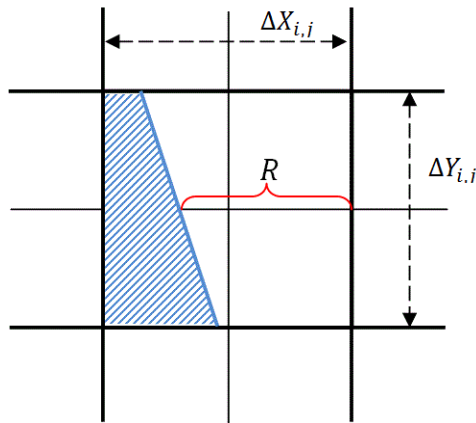


Figure 3: One orientation for the free surface where the interface line intersects both horizontal edges of the cell and one of the symmetry lines.

#### Electric field intensity

The electric field intensity on the free surface needs to be calculated to obtain the surface density of the electric charge and the electric force acting on the free surface. Again, arbitrary position of the free surface on cartesian mesh is an issue here. As shown in "Figure 4" first we find the midpoint of the approximated interface line in each cell. Then, three directions are considered: the first two being the x and y directions and the third is the direction of the line connecting the centerpoint of reconstructed interface line and center of  $(i+2,j+2)$  cell (pointed out by 'dia' subscript here as shown in "Figure 4"). Next the derivative of the electric potential is computed on these directions  $(\frac{\partial \phi}{\partial x}, \frac{\partial \phi}{\partial y}, \frac{\partial \phi}{\partial n_{Dia}})$ . As the free surface is a boundary inside the computational domain we must use directional derivative outward from the fluid interface. As shown in "Figure 4" we select three nodes in each direction (nodes specified with red colore in "Figure 4"), and compute the derivatives These nodes, however, do not lie on the center of cells thus their values are initially unknown; they are calculated by interpolating between the three points. For example to find the electric potential at the red point in cell

$(i+2,j)$  of "Figure 4", we use three green points as shown in the figure.

Having obtained the above derivatives, we need to calculate the electric field intensity vector by using two of the above derivatives depending on the values of  $f$  in adjacent cells.

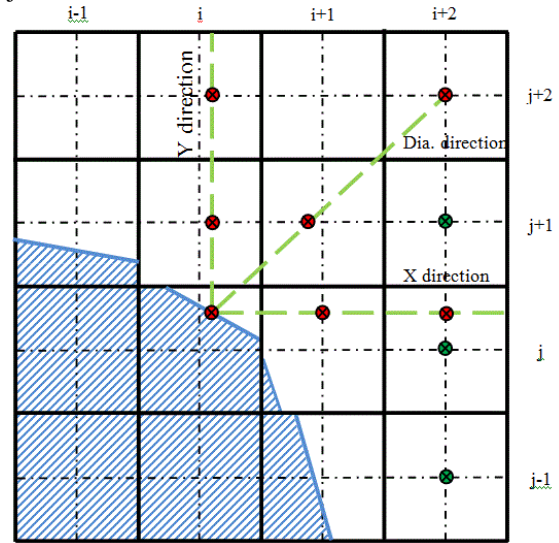


Figure 4: Nodes and directions used for the electric field intensity calculation. First, three green points are used to obtain the electric potential value at each red point. The red points are then used to calculate the potential derivative. (Only the three green points used to interpolate the potential value on the red point within cell  $(i+2,j)$  are shown in the figure.)

#### Results and Discussion

Although boundary condition capturing for Laplace equation on irregular domains is a conventional method [16] but its integration with VOF scheme is new and presented here for the first time. So to validate the formulation and the implementation of the numerical scheme, the results are compared with the analytical solutions data.

Consider a hemispherical sessile drop placed on a lower plate of a capacitor "Figure 5". The drop is conductive and has the bottom plate potential. For this case, the method of images can be used to calculate the electric field on the drop surface as [17]:

$$\frac{|\vec{E}|}{|E_\infty|} = 3 \cos \theta \quad 0 \leq \theta \leq \frac{\pi}{2} \quad (13)$$

where  $\theta$  is the polar angle measured from the drop apex, as shown in the inset of "Figure 6" and  $\vec{E}_\infty$  is the uniform electric field between plates far from the drop.

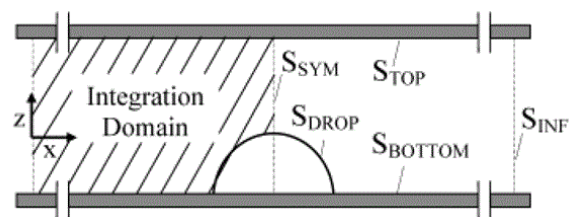


Figure 5 : A hemispherical sessile drop placed on a lower plate of a capacitor. The drop is conductive and has the same potential as that of the lower plate. [18]

Figure 6 compares the numerical and analytical electric field magnitudes and their horizontal and vertical components, calculated along the drop surface (i.e., from the apex to the contact point). The figure shows that the numerical results are in good agreement with those the analytical method, validating the numerical scheme.

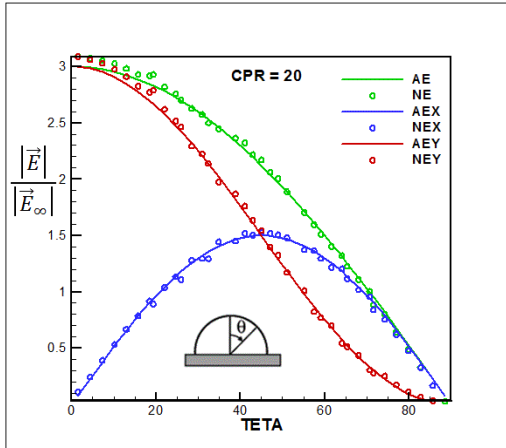


Figure 6: A comparison between analytical and numerical solutions for a hemispherical conductive drop between two conductive plates. There are 20 cells per droplet radius in this simulation (CPR = 20). E, EX and EY denote non-dimensional  $|\vec{E}|$ ,  $E_x$  and  $E_y$  respectively. The prefix A and N specify the analytical and numerical data, respectively.

#### Electrostatic atomization

The evolution of the formation of a cone-jet before atomization is illustrated in "Figure 7". We use an ellipsoid profile for free surface as initial guess; this choice is to avoid some unwanted disturbing effects. For example, if a flat profile is used, a very large and unrealistic surface tension force in the sharp edges will result.

As shown in the second image of "Figure 7", the jet is elongated due to the downwards electrostatic surface force. As the jet is elongated, the surface curvature increases at its tip and surface tension force overcomes electric force momentarily such that the jet tip returns upwards and becomes thicker. The procedure is repeated by electric force pulling the jet tip down until surface forces balance each other and jet becomes stable.

As an important point it should be noted that, similar to the surface tension force, the sharper the curvature of the free surface, the greater the electrostatic force will be. This is because the electric field intensity has a greater value as a result of a greater electric potential gradient in the sharp edges (see "Figure 9" as an example) Therefore, the electric force has the greatest value at the jet tip which is the reason of the jet break up due to a large applied potential. As the jet becomes stable, the break-up takes place at the jet tip, i.e. fine droplets form and leave the jet tip. The length scale of these droplets is very small compared to the jet diameter. Thus, it is necessary to use a very fine mesh to capture the exact characteristics of these separated droplets; this, in turn, increases the simulation time considerably. The behavior of the separated droplets, therefore, is not the focus of this study.

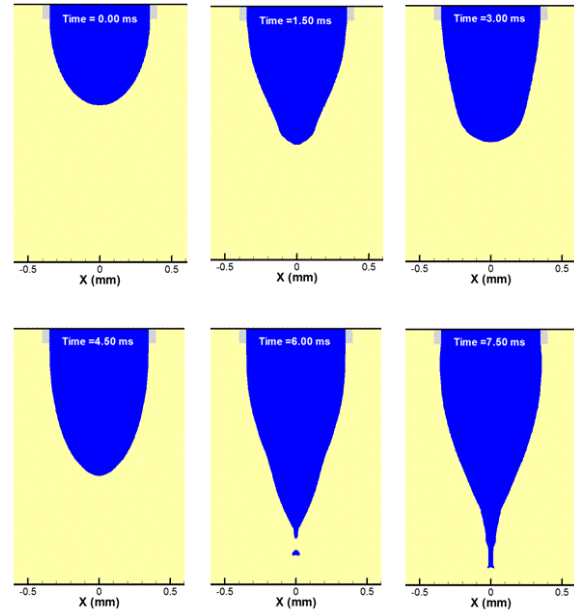


Figure 7 : The evolution of a cone-jet formation. The time associated with each image is also shown in the figure.  $\vec{V}_{Top} = -0.05 \frac{m}{s} \hat{j}$ ,  $\phi_0 = 3.7KV$

"Figure 8" shows velocity flow field. According to this figure the velocity magnitude has its maximum at the jet tip which is a consequence of the high electrostatic force on this region, as mentioned before. In addition the vortex formed in the middle of jet is apparent in this figure. As explained above the liquid jet is pulled upwards being an effect of the surface tension force. Interaction of this upward flow with the downward flow at the nozzle outlet is the cause of this vortex.

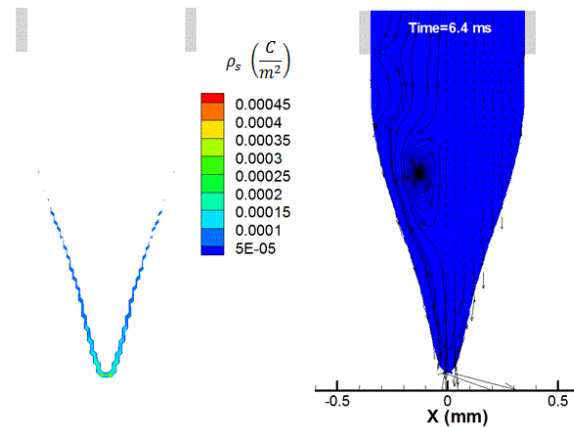


Figure 8: The velocity field (right) and surface density (left) of the electric charge at time = 6.4 ms.

The Surface charge density is also depicted in "Figure 8". It is seen that the maximum density takes place at the jet tip. This effect was expected by equation (7) where the surface charge density is proportional to electric field intensity on free surface. In other words the electric field intensity, the charge density and the electric force, all three reach their maximum value at the jet tip. Consequently the jet tip is pulled downwards. Since the nozzle flow rate is constant, as much as the jet elongates its tip gets more pointed and greater electrical force is exerted on it as a result, so its acceleration

increases. On the other hand a pointed tip has greater curvature which increases surface tension force upwards around the tip. Finally the opposite forces acting on the jet tip lead to jet break up and a little part of the tip separates in a form of a droplet. The departure of a droplet decreases the curvature at the jet tip momentarily leading to jet backstroke. The same process is repeated establishing a spray operation. The determining effect of the surface tension on the break up phenomenon should be noticed here. Assume a liquid with no surface tension, in such case velocity increase and elongation at the jet tip leads to no break up and the jet diameter at the tip approaches zero.

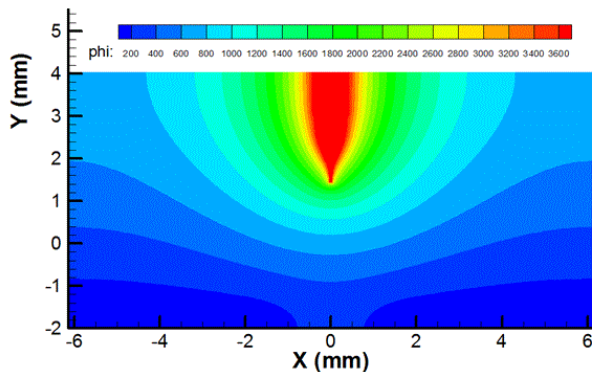


Figure 9 : The electric potential distribution for the entire domain of computation.

In "Figure 9" the electric potential distribution in whole domain is illustrated. As observed, the equipotential lines get closer at the vicinity of the jet tip demonstrating that the potential gradient is high at this region.

### Conclusions

In this study, a numerical model was developed to study the atomization of a liquid jet under an electrostatic field. The model was used to simulate the fluid flow distribution and free surface profile of a perfectly conductive liquid jet under the effect of an electric field. To validate the model, a case for which analytical results are available in the literature was considered. For a hemispherical sessile drop placed on the lower plate of a charged capacitor, the electric field intensity values on the drop free surface was obtained from the numerical model and compared to those of the analytical data. The good agreement between the two results validated the model and its underlying assumptions.

### References

[1] Jaworek, A. and Sobczyk, A.T., 2008. "Electrospraying route to nanotechnology: An overview". *Journal of Electrostatics*, 66, pp.197-219

[2] Jaworek, A. and Krupa, A., 1999. "Classification of the modes of EHD spraying". *Journal of Aerosol Science*, 30(7), pp. 873–893.

[3] Hartman, R. P. A., Borra, J. P., Brunner, D. J., Marijnissen, J. C. M., and Scarlett, B., 1999. "The evolution of electrohydrodynamic sprays produced in the cone-jet mode, a physical model". *Journal of Electrostatics*, 47, pp. 143–170.

[4] Hartman, R. P. A., Brunner, D. J., Camelot, D. M. A., Marijnissen, J. C. M., and Scarlett, B., 1999. "Electrohydrodynamic atomization in the cone-jet mode physical modeling of the liquid cone and jet". *Journal of Aerosol Science*, 30, pp. 823–849.

[5] Hartman, R. P. A., Brunner, D. J., Camelot, D. M. A., Marijnissen, J. C. M., and Scarlett, B., 2000. "Jet Break-up in electrohydrodynamic atomization in the cone-jet mode". *Journal of Aerosol Science*, 31, pp. 65–95.

[6] Alfonso, M. and Ganan-Calvo, 1998. "The surface charge in electrospraying: its nature and its universal scaling laws". *Journal of Aerosol Science*, 30, pp. 863–879.

[7] FangYan, Farouka, B. and Ko, F., 2003. "Numerical modeling of an electrostatically driven liquid meniscus in the cone-jet mode". *Journal of Aerosol Science*, 34, pp. 99-116.

[8] Zeng, J., Sobek, D., and Korsmeyer, T., "Electrohydrodynamic modeling of electrospray ionization: CAD for a  $\mu$ fluidic device – mass spectrometer interface". Flow 3D Inc.

[9] Lastowa, O., and Balachandran, W., 2006. "Numerical simulation of electrohydrodynamic (EHD) atomization", *Journal of electrostatics*, 64, pp. 850-859.

[10] Jackson, J. D., 1998. *Classical electrodynamics*. John Wiley and sons,

[11] Melcher, J. R., 1981. *Continuum electromechanics*. The MIT press,

[12] PhD thesis, Berry, S., 2008. "Electrowetting Phenomenon for Microsized fluid devices". PhD Thesis, Tufts University,

[13] Youngs D.L., 1982. "Time dependent multi material flow with large fluid distortion". *Numerical Methods for Fluid Dynamics*, pp. 273-285.

[14] Brackbill J.U., Kothe D.B., and Zang C., 1992. "A continuum method for modeling surface tension", *Journal of Computational Physics*, 100, pp. 335-354.

[15] Bussmann M., 2000. "A Three-Dimensional Model of an Impacting Droplet". Ph.D thesis, University of Toronto,

[16] Jomaa, Z., and Macaskill, C., 2005. "The embedded finite difference method for the Poisson equation in a domain with an irregular boundary and Dirichlet boundary conditions". *Journal of Computational Physics*, 202, pp. 488-506.

[17] Jeans, J., 1960. *Mathematical Theory of Electricity and Magnetism*. Cambridge University Press: Cambridge, U.K.,

[18] Bateni, A., Susnar, S. S., Amirfazli, A., and Neumann, A. W., 2004. "Development of a new methodology to study drop shape and surface tension in electric fields", *Langmuir*, 20, pp. 7589-7597